PROCEEDINGS OF SCIENCE

The Mu2e Calorimeter

L . Borrel,[a] **C. Bloise,**[b] **S. Ceravolo,**[b] **F. Cervelli,**[c] **F. Colao,**[b,d] **S. Di Falco,**[c] **E. Diociaiuti,**[b] **S. Donati,**[c] **B. Echenard,**[a] **P. Fedeli,**[b,h] **C. Ferrari,**[c,e] **A. Gioiosa,**[i] **S. Giovannella,**[b] **V. Giusti,**[c] **D. Hampai,**[b] **F. Happacher,**[b,*] **D.G. Hitlin,**[a] **M. Martini,**[b,f] **S. Middleton,**[a] **S. Miscetti,**[b] **L. Morescalchi,**[c] **D. Paesani,**[j] **D. Pasciuto,**[h] **E. Pedreschi,**[c] **F. Porter,**[a] **F. Raffaelli,**[c] **A. Saputi,**[g] **I. Sarra,**[b] **F. Spinella,**[c] **A. Zaffara**[c] **and R.Y. Zhu**[a]

[a] *California Institute of Technology, Pasadena, USA*
[b] *Laboratori Nazionali di Frascati dell'INFN,Italy*
[c] *INFN Sezione di Pisa, Pisa, Italy*
[d] *ENEA, Frascati, Italy*
[e] *CNR INO, Pisa Italy*
[f] *Department of Engineering Sciences, Guglielmo Marconi University, Rome, Italy*
[g] *INFN, Sezione di Ferrara, Ferrara, Italy*
[h] *Universitá degli Studi di Roma "La Sapienza", Roma, Italy*
[i] *Universitá degli Studi del Molise, Campobasso, Italy*
[j] *Laboratori Nazionali del Sud dell'INFN, Catania, Italy*

E-mail: fabio.happacher@lnf.infn.it

The EM CsI crystals and SiPM readout calorimeter of the Mu2e experiment is fully assembled, with all components completed and tested; the mechanical structure is fully built, with a complete integration and test of all the analog sensors and electronics. The digital electronics is being produced and installed. We summarise the Calorimeter characteristics and the assembly status, as well as the move, installation and commissioning plans of the final disks in the Mu2e hall.

42nd International Conference on High Energy Physics (ICHEP2024)
18-24 July 2024
Prague, Czech Republic

*Speaker

1. Introduction: The Mu2e experiment and Charged Lepton Flavor Violation Processes

The Mu2e experiment [1] under construction at Fermilab, will search for the Charged Lepton Flavor Violating (CLFV) process of a muon converting into an electron in the Coulomb field of Al nuclei. CLFV processes are forbidden in the Standard Model (SM) and even assuming its minimal extension, that allows neutrino oscillations, their branching ratio is completely negligible:$BR < 10^{-50}$ [2].

Any observation of CLFV processes in the muon sector will be a clear hint of New Physics. In case of no signal event observation, Mu2e plans to reach a single event sensitivity of about 3×10^{-17}, thus improving the current best limit [3] by four orders of magnitude. The experimental signature searched in Mu2e is a single electron with energy slightly below the muon rest mass, that is E_e = 104.97 MeV.

As shown in Figure 1 the Mu2e experiment is based on a system of three superconducting solenoids to enhance the number of negative muons arriving to the Stopping Target.

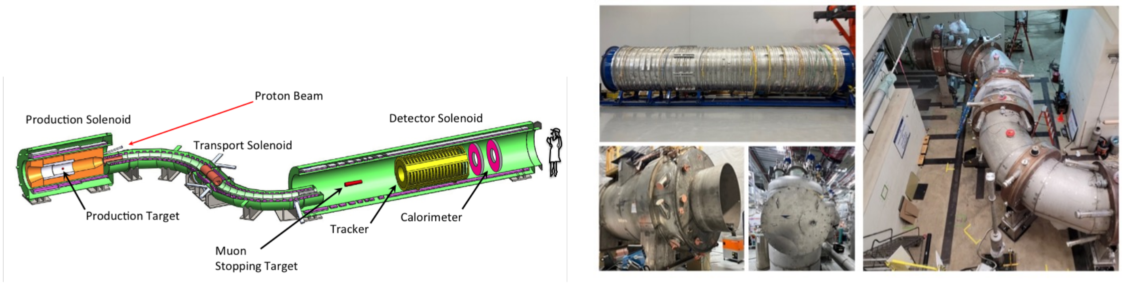

Figure 1: Left, layout of the Mu2e experiment: Production Solenoid, Transport and Detector solenoid are indicated in the picture. The Cosmic Ray Veto, surrounding the DS and part of the TS, is not shown. Right, Status of the Solenoids construction

A 8 GeV pulsed proton beam hitting the tungsten target inside the Production Solenoid (PS) produces mostly low momentum pions. Thanks to the graded magnetic field, particles produced forwards are reflected back towards the S-shaped Transport Solenoid (TS). This region allows having a very intense ($\sim 10^{10} \mu/s$) pure low-momentum negative muon beam at the entrance of the Detector 1T Solenoid (DS) thanks to a middle collimator to select the particle charge. The DS houses the stopping target (made of 37 aluminum annular 105 μm thick foils, spaced 2.2 cm apart) and the detectors - a very precise (σ_p = 200 keV at E_e) straw tubes tracker [4] and an electromagnetic calorimeter [5]. The tracker is composed of $\sim$ 20000 low mass, very thin, straw drift tubes and will measure the charged particle momenta reconstructing their trajectories in the B-field with the detected hits.

Within its lifetime the experiment plans to collect 6×10^{17} muon stops, necessary to reach its sensitivity goal. To reduce Cosmic Ray contribution, the external area of the DS, and part of the TS, are covered by a Cosmic Ray Veto (CRV) [6] system. Once muons are stopped in the Al target, they create muonic atoms and then cascade to the 1S ground state, with 39% decaying in orbit (DIO) and 61% captured by the nucleus. In the last case, due to the occuring nuclear processes, low energy protons, neutrons and photons are emitted, originating a large neutron flux as well as a large ionizing dose in the detectors. A High Purity Germanium Detector and a Lantanium Bromide Crystal constitute the Stopping Target Monitor (STM) , providing normalization to cLFV events by detecting X rays emitted from the muon capture process in the aluminum target.

To improve the current best limit by four orders of magnitude, Mu2e differs from earlier muon-to-electron conversion experiments in three major ways:

- the muon beam intensity is 10000 times greater than those of the previous experiments;
- the presence of the TS, besides providing muon sign-selection, suppresses the neutral particles contribution at the entrance of the DS, allowing an efficient muon transport to the stopping target;
- the pulsed structures of the beam and a delayed acquisition window: in order to suppress the prompt background, the muons hitting the stopping target are intended to be distributed in a narrow time burst (< 200 ns), with a bunch separation of $\sim 1.7 \mu s$ (i.e. larger than 826 ns, the muonic aluminum lifetime). Their decay products are observed only 700 ns after the proton arrival to make the prompt background negligible. These choices were guided by the observation that the result of the SINDRUM II experiment was ultimately limited by the need of suppressing the prompts.

The data-taking plan has been organized into two periods (Run I and RUN II), well separated by a two-year-long shutdown for the installation of PIP-II, the linac for the DUNE experiment. In Run I only 10% of the total number of protons on target (POT) will be produced. 75% of these POTs will be delivered with a low intensity proton beam with a mean intensity of 1.6×10^7 protons/pulse, while the remaining 25% will be delivered in the high intensity mode (3.9×10^7 protons/pulse).

2. The Mu2e Calorimeter

To validate the charged particle reconstructed by the tracker, the Mu2e calorimeter [7] provides information about its energy, timing and position, adding particle ID capabilities to reject muons and antiprotons interactions mimicking the signal. In addition, the calorimeter is required to be fast enough to provide a tracker independent software trigger and help the tracks seeding [8].

To accomplish these requirements the calorimeter has to maximise the acceptance for ~ 105 MeV/c Conversion Electron (CE) tracks, operate in vacuum, survive in the "harsh" radiation environment and satisfy the experimental requirements discussed below.

2.1 Calorimeter Requirements and Technological Choice

To fulfil the calorimeter needs, simulation guided us in defining the reconstruction requirements for 105 MeV electrons: (*i*) an energy resolution better than $\sigma_E/E = O(10\%)$, to reach a rejection factor at the level of 200 between CE and the ~ 40 MeV energy deposit from 105 MeV/c cosmic ray muons mimicking the signal [9]; (*ii*) a timing resolution better than ~ 0.5 ns, to ensure that the energy depositions in the calorimeter are in time with the conversion electrons reconstructed by the tracker and also improve the PID; (*iii*) a position resolution $\sigma_{r,z} < 1$ cm, to match the position of the energy deposit with the extrapolated trajectory of a reconstructed track; (*iv*) ability to survive the high radiation environment, maintaining its functionality for radiation exposures up to ∼ 15 krad/year in the hottest regions and for a neutron flux equivalent to 10^{12} n_{1MeV}/cm^2 / year, inside an evacuated region (10^{-4} Torr) of the DS that provides 1 T axial magnetic field; (*v*) a fast enough response in order to handle the experimental high rate ($\tau < 40$ ns); (*vi*) a temperature and gain stability within ±0.5%, not to deteriorate the energy resolution; (*vii*) reliability and redundancy to operate in vacuum for one year without any interruptions.

The final design of the Mu2e calorimeter has been distilled after a long R&D phase [10] [11] carried out to define the detector performances. It is composed of 1348 pure CsI crystals, produced by Siccas [15] and Saint Gobain [16], each one read by two custom Silicon Photo-Multipliers (SiPM's) produced by Hamamatsu [17], arranged in two annular disks. Undoped CsI represents the best compromise between cost, reliability, performance and radiation hardness, providing a fast emission time ($\tau = 30$ ns) and a sufficiently high Light Yield (∼ 2000 γ/MeV). To well match the scintillation emission of 310 nm to the SiPM Photon Detection Efficiency, UV extended SiPMs with a front window made of silicon resin were selected. Each SiPM is assembled in a Read Out Unit (ROU) connected to a Front-End Electronics (FEE) card providing pre-amplification and shaping of the signal. The FEE boards have to provide: *(i)* a signal rise time of ∼ 25 ns to allow an appropriate time reconstruction; *(ii)* a rate capability up to 1 MHz and a short fall time; *(iii)* a radiation-hardness for up to 100 krad and 10^{12} $n_{1MeV_{eq}}$/cm^2), *(iv)* a programmable bias voltage up to 200 V via a 12-bit DAC, *(v)* the possibility to set SiPM bias and to monitor current and temperature via a 12-bit ADC. The ROU is built to provide thermal dissipation and Temperature control to the SiPM and houses a fiber needle to distribute calibration laser green light to the corresponding crystal face.

The calorimeter mechanical structure was designed to support the layout of the crystals by piling them up in a self-standing array organised in consecutive staggered rows. The crystal array is supported by two coaxial cylinders. The inner cylinder must be as thin and light as possible to minimize the passive material budget in the region where spiraling background electrons are concentrated. The outer cylinder is robust enough to support the load of the crystals wrapped in a 150 μm thick foil of Tyvek® (700 kg) and the overall weight of the crates (400 kg). Each disk has two cover plates. The Source plate facing the beam is made of carbon fiber to minimize the degradation of the electron energy, while the FEE plate should also be robust to support the ROU's and embeds the copper cooling lines connected to the cooling system to maintain SiPM temperature at $\sim -10^\circ$ C to minimize the dark current; it is made of Polyether ether ketone (PEEK).

The calorimeter technological choice and the design of the custom electronics, cooling and mechanical systems were validated through an electron beam test on a large-scale crystal prototype (Module-0) [5], [13], [14] and extensive test campaigns that characterised and verified the performance of crystals, photodetectors, analogue and digital electronics. The Module-0 is composed of 51 undoped CsI crystals read out by 102 SiPM connected to FEE boards. The Module-0 was exposed to an electron beam at the Beam Test Facility of the National Laboratories of Frascati and we measured the potential performances of spatial, time and energy resolution of such a technology.

In Figure 2, the design of the calorimeter is shown: two annular disks with an inner (outer) radius of 35 cm (66 cm) paired together at a relative distance of 70 cm, corresponding to half pitch of the helical CE trajectory. Each disk is composed of 674 square based scintillating crystals of $3.4 \times 3.4 \times 20$ cm^3. Even if the crystal length is only 10 X_0, it is sufficient to contain the 105 MeV electron showers since the CEs impinge on the calorimeter surface with a $\sim 50^\circ$ angle.

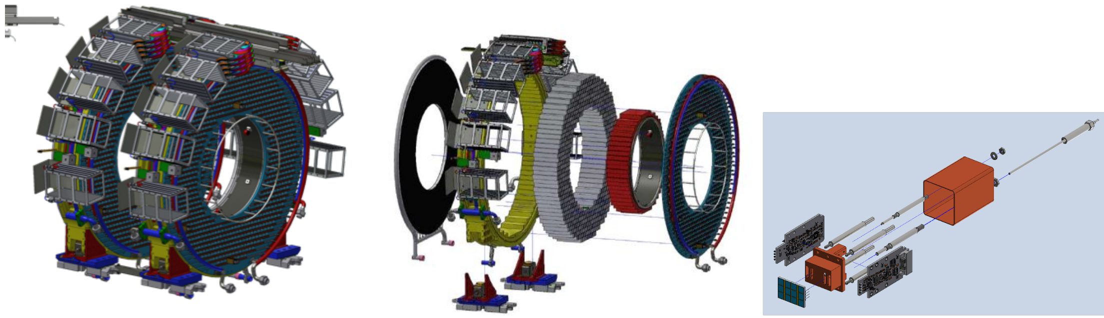

Figure 2: Calorimeter layout and Breakout of the components

The high sensitivity required by the Mu2e experiment implies a special care in detector calibration to avoid any related systematic effects. A liquid radioactive source [12] will provide an absolute energy scale and a fast response equalization between crystals. A continuous monitoring of gains and time offset for each channel is instead provided by a laser monitoring system.

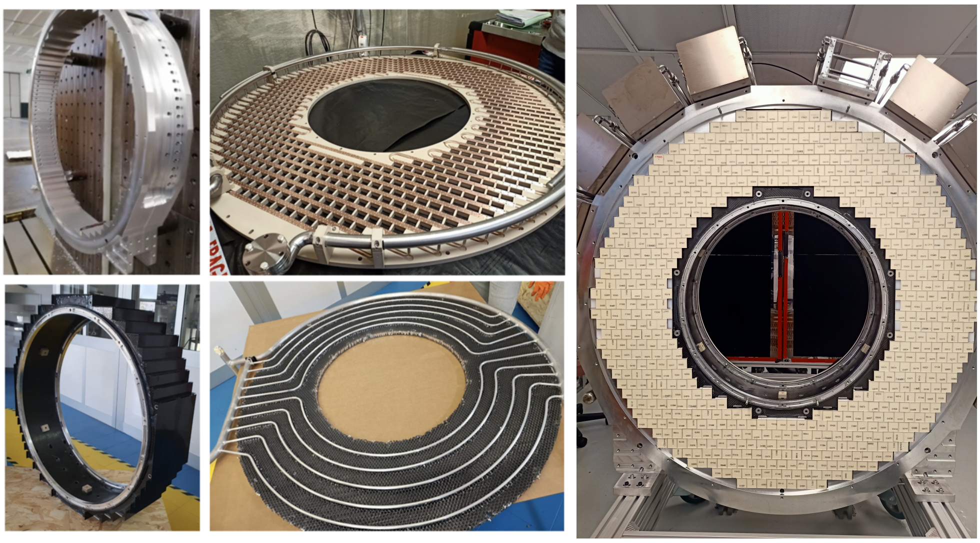

Figure 3: Calorimeter mechanical parts assembly details: (Top-left) Outer Ring, (Top-right) FEE plate, (Bottom-left) Inner Ring, (Bottom-right) Front plate with source tubing embedded in the aluminum honeycomb. Right: crystals stack and crates assembly; the crates are equipped with an onboard cooling serpentine connected to the main cooling system and a tungsten shield facing the beam.

2.2 Calorimeter Assembly Status and Commissioning

The Assembly of the Disks took place in a clean room at the Fermilab SiDet Facility. All the parts composing the Mu2e EM calorimeter have been procured and assembled in the past 3 years. In order not to spoil the DS $10-4$ Torr vacuum level, all the components making up the calorimeter disks, Crystals, ROU, MZB, DIRAC Boards, Cables etc., have been outgassed in a vacuum vessel. All the supporting mechanical parts have been assembled, the wrapped crystals have been stacked, the FEE cooling plate and the Carbon Fiber Source plate with embedded source calibration pipes are in place. All the crates have been mounted n the Outer Al ring and the piping connected and leak tested. The routing of the cables between the ROU's and the MZB is completed and we are in the process of installing the pair of MZB+Dirac boards in the crates.

As shown in Figure 4 (Left), while inserting the ROU's facing each individual crystal, we checked the health of the SiPM and FEE using a laser pulse and looking at the analog signals at the oscilloscope. Figure 4 (Right) shows the current status of the calorimeter disks.

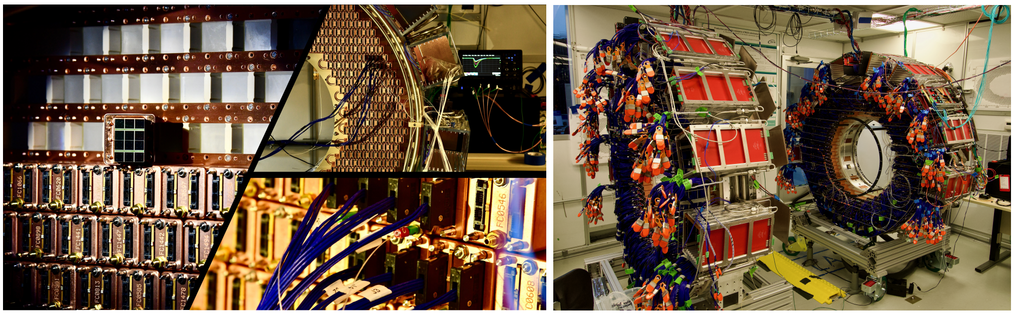

Figure 4: Left: Calorimeter's heart beating. Details of ROU insertion with SiPM facing the crystal and Analog signal at the scope. Right: The calorimeter as of August 2024.

3. Conclusions

The Mu2e Calorimeter assembly is progressing well. We plan to finish by beginning of 2025. We are designing the tools and procedure to move the disks to the Mu2e experimental hall that is 1 Mile away. Few mechanical components remain to be built, mainly cable trays to hold the bundle of HV/LV service cables and DAQ and laser fibers between the calorimeter and the Instrumentation Feedthrough Bulkhead of the Detector Solenoid. The move to the Mu2e Hall is planned for Spring 2025. In the mean time we keep testing the calo with the full DAQ chain using Cosmic and Laser runs.

Acknowledgements

We are grateful for the vital contributions of the Fermilab staff and the technical staff of the participating institutions. This work was supported by the US Department of Energy; the Istituto Nazionale di Fisica Nucleare, Italy; the Science and Technology Facilities Council, UK; the Ministry of Education and Science, Russian Federation; the National Science Foundation, USA; the National Science Foundation, China; the Helmholtz Association, Germany; and the EU Horizon 2020 Research and Innovation Program under the Marie Sklodowska-Curie Grant Agreement Nos. 734303, 822185, 858199, 101003460, and 101006726. This document was prepared by members of the Mu2e Collaboration using the resources of the Fermi National Accelerator Laboratory (Fermilab), a U.S. Department of Energy, Office of Science, HEP User Facility. Fermilab is managed by Fermi Research Alliance, LLC (FRA), acting under Contract No. DE-AC02-07CH11359.

References

[1] L. Bartoszek et al., “The Mu2e Collaboration, Mu2e technical design report,” ArXiv:1501.05241, 2015.

[2] S.M.Bilenky at al., “Lepton mixing, $\mu \to e\gamma$ decay and neutrino oscillations,” Phys. Lett. B, vol.67; pp. 309-312, 1977. 323

[3] W. Bertl, R. Engfer, E. Hermes et al., “A search for μ - e conversion in muonic gold,” Eur. Phys. J. C 47, 337–346 (2006).

[4] M. J. Lee for the Mu2e collaboration, “The straw tube tracker for the Mu2e experiment,” Nucl. Phys. B. Proc. Suppl., vol. 273-275, 325 pp. 2530-2532, 2016.

[5] N. Atanov et al., “Design and status of the Mu2e calorimeter,” IEEE-TNS 65, pp. 2073-2080, 2018, ArXiV:1802.06346.

[6] A. Artikov et al. (Mu2e CRV group), ArXiv:1511.00374 (2015).

[7]] N. Atanov et al., “The Mu2e Calorimeter Final Technical Design Report,” arXiv:1802.06341 [physics.ins-det]

[8] G. Pezzullo, P. Murat, “The calorimeter-seeded track reconstruction for the Mu2e experiment at Fermilab,” 2015 IEEE Nuclear Science Symposium and Medical Imaging Conference (NSS/MIC). IEEE, 2015.

[9] Mu2e Collaboration. “Mu2e Run I Sensitivity Projections for the Neutrinoless Conversion Search in Aluminum” Universe 9.1 (2023): 54.

[10] N. Atanov et al., “Measurement of time resolution of the Mu2e LYSO calorimeter prototype,” Nucl. Instrum. Meth. A 812, pp. 330 104-xxx, 2016.

[11] . N. Atanov et al., “Energy and time resolution of a LYSO matrix prototype for the Mu2e experiment,” Nucl. Instrum. Meth. A 824, 332 pp.684-xxx, 2016.

[12] B. Aubert et al., “The BABAR detector,” Nucl. Instrum. Meth. A 479, pp. 1-116, 2002.

[13] N. Atanov, et al., “Electron beam test of the large area Mu2e calorimeter prototype,” (2019) J. Phys. Conf. Ser. 1162, no.1, 012027.

[14] N. Atanov et al., “Design and Status of the Mu2e Crystal Calorimeter”, IEEE TNS 65 (2018) 2073-2080

[15] Siccas website, http://www.siccas.com

[16] Saint Gobain website https://www.crystals.saint-gobain.com

[17] Hamamatsu website https://www.hamamatsu.com

[18] ARTEL website www.artel-srl.com